

Relative Contact Pressure: Dependence on Surface Roughness and Vickers Microhardness

S. Song* and M. M. Yovanovich?
University of Waterloo, Waterloo, Ontario, Canada

An explicit expression for the contact hardness and the relative contact pressure is developed. This expression is simple and clearly shows the dependence of the contact hardness and the relative contact pressure upon the Vickers microhardness correlation coefficients and the surface roughness parameters. Parametric studies of the contact conductance are performed, and it is shown that theoretical predictions and experimental data are in good agreement.

Nomenclature

| | |
|------------|---|
| a_c | = mean contact radius, m |
| A_a | = apparent contact area, m ² |
| c_0, d_b | = constant for Vickers microhardness correlation |
| C | = dimensionless conductance, $C = \frac{ah}{mk_s}$ |
| d_v | = Vickers indentation diagonal, m |
| h | = conductance, W/m ² ·K |
| H_b | = bulk hardness, MPa |
| H_c | = contact microhardness, MPa |
| H_v | = Vickers microhardness, MPa |
| k | = thermal conductivity, W/m·K |
| k_s | = harmonic mean thermal conductivity, W/m·K |
| m | = mean absolute asperity slope |
| n_1, n_2 | = constants in Eqs. (20) and (21) |
| M | = gas parameter, $M = \left(\frac{2 - \alpha_1}{\alpha_1} + \frac{2 - \alpha_2}{\alpha_2} \right) \frac{2\gamma}{\gamma \mp 1} \frac{1}{Pr} \Lambda$ |
| P | = apparent contact pressure, MPa |
| Pr | = Prandtl number |
| Q | = heat flow rate, W |
| s | = constant in Eq. (18) |
| t | = local gap thickness, m |
| T | = temperature, K |
| Y | = mean plane separation, m |
| a | = thermal accommodation coefficient |
| γ | = ratio of specific heats |
| Λ | = molecular mean free path, m |
| σ | = rms surface roughness, m |

Subscripts

| | |
|-----|-------------------------|
| 1,2 | = two solids in contact |
| c | = contact |
| g | = gap |
| j | = joint |

Introduction

HEAT transfer through the interfaces formed by the mechanical contact of two solids occurs in three forms: conduction through the contacting spots, conduction through the gas-filled voids, and radiation. Under normal conditions, radiation effects are small compared to the other two and therefore can be ignored. An important geometric parameter,

Received Dec. 11, 1986; revision received March 17, 1987. Copyright © 1987 by S. Song and M. M. Yovanovich. Published by the American Institute of Aeronautics and Astronautics, Inc., with permission.

*Graduate Research Assistant, Thermal Engineering Group, Department of Mechanical Engineering.

†Professor of Mechanical Engineering, Thermal Engineering Group, Department of Mechanical Engineering. Associate Fellow AIAA.

which controls the rate of heat transfer through the contacting spots, is the ratio of actual to apparent areas of contact. This area ratio is determined by the relative contact pressure, defined as the ratio of the applied pressure to the contact microhardness. The relative contact pressure also influences the effective thickness of the layers of gas entrapped in the interface voids and thus directly affects the rate of gas conduction. A firm understanding of the nature of the relative contact pressure, therefore, is a prerequisite for studying the phenomenon of contact heat transfer.

For contacts of nominally flat but microscopically rough surfaces, Yovanovich et al.¹ developed an implicit geometric/mechanical model that relates relative contact pressure with surface roughness characteristics and Vickers microhardness test results. This model allows one to estimate, through iterations, the contact microhardness and the relative contact pressure and thus to predict the rate of heat transfer across the interface. An explicit expression for relative contact pressure is now available, and it is the purpose of this paper to present its development. The explicit expression not only simplifies the calculation for contact heat-transfer prediction but readily reveals the quantitative relationships between the dependent and independent parameters. The latter part of this paper contains the analysis and verification, through experimental data, of the effects of various parameters on contact heat transfer.

Review of Contact Conductances and Relative Contact Pressure

Contact, Gap, and Joint Conductance

Heat transfer through the interface of two nominally flat surfaces when radiation effects are neglected takes the following form:

$$Q_j = Q_c + Q_g \quad (1)$$

where Q_c , Q_g , Q_j are the rate of heat transfer through the total real contact area, the rate of heat transfer through the interstitial gas layer, and the total heat transfer, respectively. The conductance coefficients are introduced in the same manner as the film coefficient in convection heat transfer:

$$\begin{aligned} h_c &= \frac{Q_c/A_a}{AT} \\ h_g &= \frac{Q_g/A_a}{AT} \\ h_j &= \frac{Q_j/A_a}{\Delta T} \end{aligned} \quad (2)$$

where h_c , h_g , h_j are the coefficients of contact, gap, and joint conductance, respectively, AT is the effective temperature

difference across the interface, and A , is the apparent contact area. One can use A , for A , in the definition of gap conductance because the gap area is approximately equal to the apparent contact area. Dimensionless conductances are, then, defined as

$$\begin{aligned} C_c &= \frac{\sigma h_c}{m k_s} \\ C_g &= \frac{\sigma h_g}{m k_s} \\ C_j &= \frac{\sigma h_j}{m k_s} \end{aligned} \quad (3)$$

where C_c , C_g , C_j are the dimensionless contact, gap, and joint conductances, respectively. The parameters a , m , k_s are, respectively, the effective rms surface roughness, the mean absolute asperity slope, and the harmonic mean thermal conductivity of the two contacting solids. In terms of dimensionless conductances, Eq. (1) reduces to

$$C_j = C_c + C_g \quad (4)$$

Yovanovich¹ developed a simple, accurate correlation for the contact conductance model:

$$C_c = \frac{\tilde{h}^c}{m k_s} = 1.25 \left(\frac{P}{H_c} \right)^{0.95} \quad (5)$$

where P is the apparent contact pressure and H_c is the contact microhardness of the softer surface. This expression for contact conductance is valid for $10^{-6} \leq P/H_c \leq 2.3 \cdot 10^{-2}$, and its agreement with experimental data was verified by Hegazy.³

Yovanovich et al.⁵ also developed a gap conductance model that takes into consideration the statistical nature of the roughness of the contacting surfaces and the behavior of gases in very small gaps:

$$h_g = \frac{k_g}{\sigma \sqrt{2\pi}} \int_0^\infty \frac{\exp\left[-\left(\frac{Y-t}{\sigma}\right)^2/2\right]}{\frac{t}{\sigma} + \frac{M}{\sigma}} d\left(\frac{t}{\sigma}\right) \quad (6)$$

where k_g , Y , and t are the gas conductivity, the mean plane separation, and the local gap thickness, respectively. The gas parameter M is defined as

$$M = \left(\frac{2-\alpha}{\alpha} \quad 2-\alpha \quad \frac{2\gamma}{\gamma+1} \quad \frac{1}{Pr} \right) \quad (7)$$

where α_1 and α_2 are the thermal accommodation coefficients of the two surfaces and γ , Pr , and Λ are the ratio of specific heats, the Prandtl number, and the molecular mean free path, respectively. The mean plane separation Y is related to the relative contact pressure P/H_c by²

$$\frac{Y}{\sigma} = \sqrt{2} \operatorname{erfc}^{-1} \left(\frac{2P}{H_c} \right) \quad (8)$$

Relative Contact Pressure and Contact Microhardness

Relative contact pressure is defined as P/H_c , the ratio of apparent applied pressure to contact microhardness. Its influence on contact heat transfer is clearly exhibited by Eqs. (5), (6), and (8). Physically, the ratio P/H_c controls three geometric elements important in contact heat transfer: contact spot density, mean contact spot radius, and separation distance of the mean planes of the two contacting surfaces.

Contact microhardness H_c by itself depends on several parameters: mean surface roughness, mean absolute slope of

asperities, type of material, method of surface preparation, and applied pressure. Sufficient information regarding the type of material and the surface hardness characteristics can be introduced into the calculation of relative contact pressure in the form of Vickers microhardness correlations corresponding to a range of contact pressures. Vickers microhardness tests are performed for a range of indentation diagonals. Typical results of such tests for several different materials are shown in Fig. 1. The results of Vickers hardness tests can be correlated in a power form:^{3,4}

$$\frac{H_v}{H_b} = \left(\frac{d_v}{d_b} \right)^{c_0} \quad (9)$$

where H_v is Vickers microhardness, H_b bulk hardness, d_v mean indentation diagonal, and c_0 , d_b the correlation coefficients. The correlation coefficient d_b has the unit of length and may be interpreted as representing a characteristic length in the form of Vickers indentation diagonal, above which the microhardness is essentially the bulk hardness H_b . Thus, d_b depends upon both the bulk hardness and the microhardness characteristics of the material and also upon the choice of the functional form for the correlation.

In the computation of contact microhardness, an assumption is made that the contact microhardness of the surface being penetrated by the asperities of the harder surface is the same as the Vickers microhardness corresponding to the equivalent Vickers indentation diagonal:^{1,3,4}

$$\frac{H_c}{H_b} = \left(\frac{d_v}{d_b} \right)^{c_0} \quad (10)$$

and

$$d_v = \sqrt{2\pi} a_c \quad (11)$$

where a_c is the mean contact spot radius in m. The mean contact spot radius, in turn, is related to the relative mean plane separation, Y/σ :⁶

$$a_c = \sqrt{\frac{8}{\pi}} \frac{\sigma}{m} \exp\left(\frac{Y}{\sqrt{2}\sigma}\right)^2 \operatorname{erfc}\left(\frac{Y}{\sqrt{2}\sigma}\right) \quad (12)$$

As mentioned previously, the relative mean plane separation depends upon the relative contact pressure, as shown in Eq. (8). Finally, Eqs. (8) and (10-12) form a set of four nonlinear equations that define a unique value of H_c . Once the values for

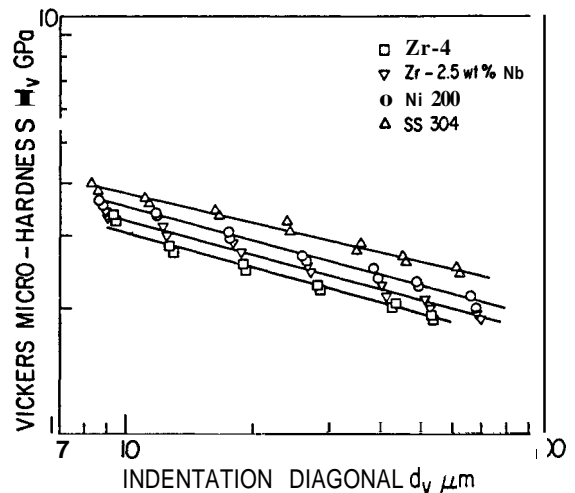


Fig. 1 Vickers microhardness variation of different materials with indentation diagonal?

$P, H_b, c_0, d_b,$ and σ/m are given, this set of equations can be solved by iteration for H_c or P/H_c .

It is evident from this brief review that the implicit formulation does not permit one to ascertain directly the effect of the contact pressure, surface roughness parameters, and Vickers microhardness correlations upon the contact and gap conductances. Any parametric study of the joint conductance requires the computation of the contact and gap conductances, which requires iteration upon the relative contact pressure. It is therefore necessary to develop an explicit relationship that will permit direct computation of the relative contact pressure and the joint conductance. The explicit expression will give additional physical insights into the effect of the pressure, surface roughness parameters, and Vickers microhardness distribution upon the relative contact pressure. It will also allow one to compute efficiently the relative contact pressure whenever it is required.

Explicit Expression for Relative Contact Pressure

Explicit Expression Development

Equations (8) and (10-12) can be combined to result in the following implicit equation for the relative contact pressure, P/H_c :

$$\frac{P}{H_c} = \frac{P}{H_b} \left[\frac{4\sigma}{md_b} \right]^{-c_0} \left[\exp \left\{ \left(\operatorname{erfc}^{-1} \left(\frac{2P}{H_c} \right) \right)^2 \right\} \left(\frac{2P}{H_c} \right) \right]^{-c_0} \quad (13)$$

Collecting terms and taking the natural logarithm of both sides, the equation becomes

$$\ell_n \left(\frac{P}{H_c} \right) + \frac{c_0}{c_0 + 1} \left\{ \operatorname{erfc}^{-1} \left(\frac{2P}{H_c} \right) \right\}^2 = \frac{1}{c_0 + 1} \ell_n \left\{ \frac{P}{H_b} \left(\frac{8\sigma}{md_b} \right)^{-c_0} \right\} \quad (14)$$

The $\operatorname{erfc}^{-1}(2P/H_c)$ term in Eq. (14) is approximated by the following accurate expression:

$$\operatorname{erfc}^{-1} \left(\frac{2P}{H_c} \right) \approx 0.9638 \left[-\ell_n \left(5.589 \frac{P}{H_c} \right) \right]^{\frac{1}{2}} \quad (15)$$

This approximation is accurate to the maximum relative error of 2% for the range $10^{-6} \leq P/H_c \leq 2 \cdot 10^{-2}$ (see Table 1). Finally, substituting Eq. (15) for $\operatorname{erfc}^{-1}(2P/H_c)$ in Eq. (14) and manipulating terms leads to the following explicit expression:

$$\frac{P}{H_c} = \left[\frac{P}{H_b \left(\frac{1.62\sigma}{md_b} \right)^{c_0}} \right]^{1/(1+0.071c_0)} \quad (16)$$

which is valid for $10^{-6} \leq P/H_c \leq 2 \cdot 10^{-2}$. Equation (16) clearly reveals the quantitative dependence of the relative contact pressure upon the geometric and mechanical parameters $\sigma, m, c_0, d_b, H_b,$ and P . The relative contact pressure depends on the apparent pressure as $P/H_c \propto P^{1/(1+0.071c_0)}$. It is interesting to note that the parameters $\sigma, m, H_b,$ and d_b appear with c_0 as a group, $H_b(1.62\sigma/md_b)^{c_0}$. This term, in comparison with Eq. (10), may be thought of as some characteristic microhardness representing the specific surface condition of a work-hardened material. The relative contact pressure is related to this characteristic microhardness in conjunction with the apparent pressure by the power coefficient $1/(1+0.07c_0)$. Equation (16) also suggests that for materials with $c_0 = 0$ (such as some annealed aluminum alloys), the contact microhardness is the same as the bulk hardness H_b .

Comparison of Explicit Approximation with Implicit Iterative Expression

Differences in the calculation of relative contact pressure by the two expressions arise solely from the approximation made

for the inverse complementary error function, $\operatorname{erfc}^{-1}(2P/H_c)$. In this section, the two expressions will be compared for the calculation of relative contact pressures P/H_c , contact conductance C_c , and relative mean plane separation Y/σ . To simplify the task of the comparison, some reduction in the number of parameters can be made. Hegazy³ showed that the power coefficient c_0 of the Vickers microhardness correlation for a number of materials he studied can be fixed to a value of -0.26 without introducing a significant error. Table 2 shows typical values of $H_b, d_b,$ and c_0 obtained for several different materials. Also, Eq. (16) suggests that the remaining five parameters may be grouped into two: P/H_b and σ/md_b .

Table 1 Accuracy of $\operatorname{erfc}^{-1}(2P/H_c)$ approximation

| P/H_c | $\operatorname{erfc}^{-1}(2P/H_c)$ | Eq. (15) | % diff. |
|-------------------|------------------------------------|----------|---------|
| $1 \cdot 10^{-6}$ | 3.362 | 3.352 | 0.3 |
| $5 \cdot 10^{-6}$ | 3.123 | 3.121 | 0.1 |
| $1 \cdot 10^{-5}$ | 3.016 | 3.017 | 0.0 |
| $5 \cdot 10^{-5}$ | 2.751 | 2.757 | -0.2 |
| $1 \cdot 10^{-4}$ | 2.630 | 2.638 | -0.3 |
| $5 \cdot 10^{-4}$ | 2.327 | 2.337 | -0.5 |
| $1 \cdot 10^{-3}$ | 2.185 | 2.195 | -0.5 |
| $5 \cdot 10^{-3}$ | 1.822 | 1.823 | -0.1 |
| $1 \cdot 10^{-2}$ | 1.645 | 1.637 | 0.5 |
| $2 \cdot 10^{-2}$ | 1.452 | 1.427 | 1.8 |

Table 2 Vickers microhardness correlations, $H_v/H_b = (d_v/d_b)^{c_0}$,^{3,4}

| Material | H_b MPa | $d_b \times 10^6$, m | c_0 | % diff. | |
|-------------|--------------|--------------------------|-------|---------|-----|
| | | | | max | rms |
| Zr-4 | 1913 | 53 | -0.26 | 3.9 | 1.8 |
| Zr-2.5wt%Nb | 1727 | 102 | -0.26 | 9.7 | 2.7 |
| Ni200 | 1668 | 157 | -0.26 | 5.2 | 1.8 |
| SS304 | 1427 | 387 | -0.26 | 5.9 | 2.4 |

Table 3 Percent difference of P/H_c ($c_0 = -0.26$)

| P/H_b | $\sigma/(md_b)$ | | | | |
|-----------|-----------------|-----------|-----------|--------|--------|
| | 10^{-3} | 10^{-2} | 10^{-1} | 10^0 | 10^1 |
| 10^{-6} | -3.3 | -2.8 | -2.2 | -1.7 | -1.2 |
| 10^{-5} | -1.3 | -0.8 | -0.4 | 0.0 | 0.4 |
| 10^{-4} | 0.3 | 0.7 | 0.9 | 1.1 | 1.3 |
| 10^{-3} | 1.3 | 1.3 | 1.3 | 1.2 | 1.0 |
| 10^{-2} | 1.0 | 0.6 | 0.1 | -0.7 | -1.8 |

Table 3 shows the percent difference in the values of relative contact pressure computed by the two expressions. The maximum difference is -3.3% and occurs when $P/H_b = 10^{-6}$ and $\sigma/md_b = 10^{-3}$. In most practical cases, however, the difference is less than 2%. The range of σ/md_b chosen represents the practical range of $\sigma, 0.1-50 \times 10^{-6}$ m, and $m, 0.05-0.2$ for conforming rough surfaces.

Table 4 shows the difference in predicted values of contact conductance C_c using Eq. (5). Again, the maximum difference occurs at $P/H_b = 10^{-6}$ and $\sigma/md_b = 10^{-3}$, and in general, the difference is less than 2%.

The difference in the predicted values of relative mean plane separation Y/σ is even smaller, as shown in Table 5. In all cases examined, the difference is less than 1%.

Table 4 Percent difference of C_c ($c_0 = -0.26$)

| P/H_b | 10^{-3} | 10^{-2} | 10^{-1} | 10^0 | 10^1 |
|-----------|-----------|-----------|-----------|--------|--------|
| 10^{-6} | -3.2 | -2.6 | -2.1 | -1.6 | -1.1 |
| 10^{-5} | -1.2 | -0.8 | -0.4 | 0.0 | 0.4 |
| 10^{-4} | 0.3 | 0.6 | 0.9 | 1.1 | 1.2 |
| 10^{-3} | 1.2 | 1.3 | 1.3 | 1.2 | 0.9 |
| 10^{-2} | 1.0 | 0.6 | 0.1 | -0.7 | -1.7 |

Table 5 Percent difference of Y/σ ($c_0 = -0.26$)

| P/H_b | $\sigma/(md_b)$ | | | | |
|-----------|-----------------|-----------|-----------|--------|--------|
| | 10^{-3} | 10^{-2} | 10^{-1} | 10^0 | 10^1 |
| 10^{-6} | 0.1 | 0.1 | 0.1 | 0.1 | 0.1 |
| 10^{-5} | 0.1 | 0.0 | 0.0 | 0.0 | 0.0 |
| 10^{-4} | 0.0 | 0.0 | -0.1 | -0.1 | -0.1 |
| 10^{-3} | -0.1 | -0.1 | -0.1 | -0.1 | -0.1 |
| 10^{-2} | -0.1 | -0.1 | 0.0 | 0.1 | 0.4 |

Dependence of Contact Conductance upon Surface and Microhardness Parameters

Theoretical Prediction

The explicit expression for relative contact pressure, Eq. (16), makes it possible to readily examine the effect of its parameters on contact conductance. Substituting Eq. (16) for P/H_c in Eq. (5) yields a contact conductance expression in terms of measurable surface and mechanical parameters:

$$C_c = \frac{h_c \sigma}{k_s m} = 1.25 \left[\frac{P}{H_b (1.62 \sigma / md_b)^{c_0}} \right]^{0.95/(1+0.071c_0)} \quad (17)$$

Defining for convenience, $s = 0.95/(1+0.071c_0)$, we obtain

$$\frac{h_c}{k_s} = 1.25 \left(\frac{1.62}{d_b} \right)^{-c_0 s} \left(\frac{P}{H_b} \right)^s \left(\frac{\sigma}{m} \right)^{-(c_0 s + 1)} \quad (18)$$

As mentioned previously, for a number of materials c_0 , one of the two Vickers microhardness correlation coefficients can be set to a value of -0.26 ,³ and thus, $s = 0.97$ and $c_0 s = -0.25$. Then, Eq. (18) reduces to the semigeneral expression

$$\frac{h_c}{k_s} = \frac{1.13}{d_b^{0.25}} \left(\frac{P}{H_b} \right)^{0.97} \left(\frac{\sigma}{m} \right)^{-0.75} \quad (19)$$

The contact conductance, as one would expect, increases with the applied contact pressure. Equation (19) predicts that for the materials with $c_0 = -0.26$, the power index for the proportionality of h_c with respect to P is 0.97. The contact conductance also increases with the mean asperity slope but decreases with the rms roughness at the power index of 0.75.

Verification of Pressure Dependence by Experimental Data

For a given material and surface characteristics (H_b , d_b , σ , m), the contact conductance would be directly proportional to the applied contact pressure, and the degree of dependence may be approximately expressed as

$$\frac{h_c}{k_s} \propto P^{n_1} \quad (20)$$

Equation (19) predicts the power constant n_1 to be equal to $s = 0.97$ for materials with $c_0 = -0.26$. Table 6 shows the values of n_1 obtained from the experimental data by Hegazy.³ It is

seen from the table that the values of n_1 obtained for the four different materials (Nickel 200, Stainless Steel 304, Zircaloy-4, Zr-2.5wt%Nb) for the range of σ/md_b , 0.01–1 and P/H_b , 2×10^{-4} – 5×10^{-3} agree quite well with the predicted value of 0.97. Estimates of n_1 from the contact conductance data reported by other authors are also in agreement with the predicted value; these are shown in Table 7.

Verification of Surface Roughness Dependence by Experimental Data

For a given material and under a specific contact pressure, the dependence of contact conductance on surface roughness parameters can be approximately expressed as

$$\frac{h_c}{k_s} \propto \left(\frac{\sigma}{m} \right)^{n_2} \quad (21)$$

Theory predicts, according to Eq. (18), that $n_2 = -(c_0 s + 1)$, and thus, for materials with $c_0 = -0.26$, the power coefficient n_2 is -0.75 . The values of n_2 obtained from the experimental data of Hegazy³ are shown in Table 8. Again, the agreement between the predicted and experimental values is found to be very good.

Table 6 Experimental values of power constant n_1 ³

| Contact materials | Power constant n_1 |
|-------------------|----------------------|
| Ni200 pair | 0.95 |
| SS304 pair | 0.97 |
| Zr-4 pair | 0.94 |
| Zr-2.5wt%Nb pair | 0.95 |

Table 7 Power constant n_1 obtained from various authors

| Contact materials | Power constant n_1 | Authors |
|-----------------------|----------------------|-------------------------------|
| UO ₂ –Zr-2 | 0.93 | Ross and Stoute ⁷ |
| Aluminum pair | 0.95 | Boeschoten and |
| Al–Fe | 0.99 | Van Der Held ⁸ |
| Steel pair | 0.97 | Shykov and Ganin ⁹ |
| Duralumin pair | 0.94 | |
| Copper pair | 1.05 | |

Table 8 Experimental values of power constant n_2 ³

| Contact materials | Power constant n_2 |
|--------------------------|----------------------|
| Nickel 200 pair | -0.76 |
| Stainless Steel 304 pair | -0.77 |
| Zircaloy-4 pair | -0.76 |
| Zr-2.5wt%Nb pair | -0.75 |

Conclusions

An explicit expression for relative contact pressure that considerably simplifies the prediction of contact heat transfer has been developed. The difference in the computed values of relative contact pressure between the implicit and the explicit expressions is negligible. Furthermore, the explicit expression allows parametric studies of contact heat transfer. The parametric study performed on contact conductance shows that theoretical predictions and experimental data are in good agreement.

Acknowledgments

The authors acknowledge the financial support of the Natural Sciences and Engineering Research Council of Canada under operating grant **A1455** for **Dr. Yovanovich**.

References

- ¹Yovanovich, M. M., Hegazy, A. H., and DeVaal, J., "Surface Hardness Distribution Effects Upon Contact, Gap and Joint Conductances," AIAA Paper 82-0887, 1982.
- ²Yovanovich, M. M., "Thermal Contact Correlations," *Spacecraft Radiative Transfer and Temperature Control*, Progress in Astronautics and Aeronautics, Vol. 83, edited by T. E. Horton, AIAA, New York, 1982.
- ³Hegazy, A. A., "Thermal Joint Conductances of Conforming Rough Surfaces: Effects of Surface Micro-Hardness Variation," Ph.D Thesis, Department of Mechanical Engineering, University of Waterloo, Ontario, Canada, 1985.

⁴Song, S., "Dimensionless Expression for Vickers Microhardness Correlation," Rept. MHTL-CR/SS02, Microelectronics Heat Transfer Laboratory, Department of Mechanical Engineering, University of Waterloo, Ontario, Canada, 1987.

⁵Yovanovich, M. M., DeVaal, J., and Hegazy, A. A., "A Statistical Model to Predict Thermal Gap Conductance Between Conforming Rough Surfaces," AIAA Paper 82-0888, 1982.

⁶Mikic, B. B., "Analytical Studies of Contact of Nominally Flat Surfaces; Effect of Previous Loading," *Journal of Lubrication Technology*, Vol. 93, No. 4, 1971, pp. 451-459.

⁷Ross, A. M. and Stoute, R. L., "Heat Transfer Coefficient between UO₂ and Zircaloy-2," Rept. CRFD-1075, Atomic Energy of Canada Ltd., Chalk River, Ontario, Canada, June 1962.

⁸Boeschoten, F. and Van Der Held, E. F. M., "The Thermal Conductance of Contacts between Aluminum and Other Metals," *Physica*, Vol. 23, 1957, pp. 37-44.

⁹Shlykov, Y. U. P. and Ganin, Y. E. A., "Thermal Resistance of Metallic Contacts," *International Journal of Heat and Mass Transfer*, Vol. 1, 1964, pp. 921-929.

From the AIAA Progress in Astronautics and Aeronautics Series...

FUNDAMENTALS OF SOLID-PROPELLANT COMBUSTION – v. 90

*Edited by Kenneth K. Kuo, The Pennsylvania State University
and
Martin Summerfield, Princeton Combustion Research Laboratories, Inc.*

In this volume distinguished researchers treat the diverse technical disciplines of solid-propellant combustion in fifteen chapters. Each chapter presents a survey of previous work, detailed theoretical formulations and experimental methods, and experimental and theoretical results, and then interprets technological gaps and research directions. The chapters cover rocket propellants and combustion characteristics; chemistry ignition and combustion of ammonium perchlorate-based propellants; thermal behavior of RDX and HMX; chemistry of nitrate ester and nitramine propellants; solid-propellant ignition theories and experiments; flame spreading and overall ignition transient; steady-state burning of homogeneous propellants and steady-state burning of composite propellants under zero cross-flow situations; experimental observations of combustion instability; theoretical analysis of combustion instability and smokeless propellants.

For years to come, this authoritative and compendious work will be an indispensable tool for combustion scientists, chemists, and chemical engineers concerned with modern propellants, as well as for applied physicists. Its thorough coverage provides necessary background for advanced students.

Published in 1984, 891 pp., 6 x 9 illus. (some color plates), \$69.95 Mem., \$99.95 List; ISBN 0-915928-84-1

TO ORDER WRITE: Publications Dept., AIAA, 370 L'Enfant Promenade S.W., Washington, D.C. 20024-2518